Some Implementation Details of Production Data Integration by Numerical Calculation of Sensitivity Coefficients

Linan Zhang

Centre for Computational Geostatistics
University of Alberta

Abstract

This short note presents some implementation aspects of the methodology proposed in the preceding two papers. The effects of perturbation location, number of perturbation locations and the variogram used to propagate perturbations have been looked at. The calculation of the sensitivity coefficients and the goodness of the linear approximation of pressure and oil production rates are also considered. Some ideas for future work are identified.

Perturbation Location, Perturbation Number, Propagation Variogram and Range

The original base model was updated by the proposed methodology with one perturbation location at each iteration, a perturbation range of 4 grid blocks and a spherical variogram. The perturbation location was selected in each iteration by two ways. The first approach was to select the perturbation location partly based on the local mismatch at the well locations with a small stochastic deviation. The results are shown in Figure 1. The second approach was to simply select the well location with the largest product of the local mismatch and the fractional flow rate at the well locations. The results of global mismatch are shown in Figure 2. The two sets of perturbation locations are shown in Table 1. The global mismatch decreased the most with the second alternative.

Figure 2 shows the large difference of mismatch for the two sets of perturbation locations during iterations 4 to iteration 7, which is because the locations are quite different. After iteration 8, the mismatch values corresponding to the two sets of perturbation locations are very close although the perturbation locations are not same. Therefore the perturbation location has a larger effect on the global mismatch early in the procedure. We do not understand the interesting behavior at iteration 4 where the perturbation at the grid block with Well 8 led to a significant improvement.

The perturbations were propagated to the whole grid system by simple kriging with a range of 4 grid blocks and variogram of spherical type and Gaussian type, respectively. The perturbation locations in each iteration were selected at the well locations with the mismatch over 0.08 for multiple perturbations at each iteration. The grid block with the largest production of the local mismatch and oil rate mismatch at wells was set as the perturbation location for single perturbation at each iteration. The mismatch results are shown in Figure 3 and relevant perturbation locations are shown in Table 2 and Table 3.

The results in Figure 3 shows that the multiple perturbations at each iteration make the methodology more efficient and the perturbation variogram has a larger effect on the results for one perturbation than for multiple perturbations. Multiple perturbations at each iteration and Gaussian type variogram should be more efficient for the methodology. The mismatch for the

updated model after the fifth iterations reached the mismatch level for the updated model after the 10th iterations in case of one perturbation location in each iteration.

Ranges of 3, 4, 5 and 6 grid blocks were selected in the study and the results are shown in Figure 4. Multiple perturbation locations were selected in each iteration and Gaussian variogram was selected for propagating the perturbations. It can be seen from Figure 4 that the range of 5 grid blocks is the best, which is about the minimum well spacing.

Sensitivity Coefficients

Sensitivity coefficients of pressure and production rate relative to the property change are very important in the methodology. The behavior of the sensitivity coefficients at Well 1 will be looked at in more detail. Well 1 started as a producer and was recently converted into an injector. The perturbation locations, perturbation ranges and perturbation factors are same for the two iterations being considered. The results are shown in Figure 5. We can see that the sensitivity coefficients at the well in the production period change with time and decline in magnitude with iteration. The change of sensitivity coefficients with pressure in the injection period is more complicated.

The effect of perturbation variogram type on sensitivity coefficients was studied. The results are shown in Figure 6. We can see that the perturbation variogram has a larger effect on the sensitivity coefficients of oil production rate than on the sensitivity coefficients of the well bottom hole pressure.

Linear Approximation of Reservoir Behavior

The linearized formula of reservoir behavior (pressure and flow rate) with the property change is an assumption used for optimization in the methodology. The scatter plots of the calculated results from the linearized formulas vs. the simulation results at the first two iterations of one application are shown in Figure 7. The data in the figure were selected at all wells corresponding to the observed data. It shows that the reservoir behaviors obtained by means of the linear approximation and flow simulation are consistent, which means that using the linear approximation of reservoir behavior in the optimization of the proposed methodology is suitable.

Relative Permeability Curves

Based on the two phase radial flow without considering capillary pressure and gravity for incompressible or slightly compressible liquids, the following equations can be derived.

For pressure:

$$\frac{\Delta p_{w,t,m}}{\Delta p_{w,t,total}} = \frac{\Delta \bar{k}_m}{\bar{k} + \Delta \bar{k}_m} \times \frac{\bar{k} + \sum_{m=1}^{n_m} \Delta \bar{k}_m}{\sum_{m=1}^{n_m} \Delta \bar{k}_m}$$

For oil production rate

$$\frac{\Delta q_{w,t,m}}{\Delta q_{w,t,total}} = \frac{\Delta \bar{k}_{rom}}{k_{ro}(\bar{s}_w)} \times \frac{k_{ro}(\bar{s}_w)}{\sum_{m=1}^{n_m} \Delta \bar{k}_{rom}} = \frac{\Delta \bar{k}_{rom}}{\sum_{m=1}^{n_m} \Delta \bar{k}_{rom}}$$

where $\Delta p_{w,t,m}^{i}$ and $\Delta q_{w,t,m}^{i}$ refer to the changes of pressure and fractional flow rate at the well with the index w at the time step t introduced by the perturbation at the location $\mathbf{u}_m$ without considering the other perturbations; $\Delta p_{w,t,total}^{i}$ and $\Delta q_{w,t,total}^{i}$ refer to the changes of pressure and fractional flow rate at the well with the index w at the time step t introduced by the joint perturbations at all perturbation locations; $\bar{k}$ is the average permeability in the area around the well; $\Delta \bar{k}_m$ is the change of the average permeability in the area around the well introduced by the permeability change at the location $\mathbf{u}_m$; n_m is the number of master point locations; $k_{ro}(\bar{s}_w)$ is the average relative permeability of oil at the time step t in the area around the well; $\Delta \bar{k}_{rom}$ is the change of the average relative permeability of oil at time step t in the area around the well introduced by the permeability change at the location $\mathbf{u}_m$.

From the above equations, we can see that the pressure difference has no relationship with relative permeability curves. Therefore, relative permeability curves can only affect sensitivity coefficients of rate.

Average Permeability around Wells

The methodology was applied to two different realizations generated by geostatistical technique. The iteration stopped when the updated models could not be improved significantly. The average values of the average permeability in the reservoir were calculated and plotted in Figure 8. The average permeabilities for in the area around the wells are very close when we use a range of about 2.8. This is one of the common features between the updated models. Additional work is required to verify that this is a common feature over many realizations. If it were, then we could build this feature into the initial reservoir models.

Conclusions and Future Work

The sensitivity coefficients change with time and iteration. The linearized formula to get the optimal property changes at all master point locations appears valid. The locations chosen for perturbation have a large effect on the mismatch results. Selecting multiple locations per iteration speeds convergence.

There are some areas for future work. The methodology is very dependent on reasonable sensitivity coefficients and the linearized approximation to the flow equations. Additional work is needed to establish sensitivity coefficients that better account for the interaction between wells for the reliable calculation of sensitivity coefficients when the multiple locations are perturbed simultaneously.

Additional research is also needed to develop procedures to find the common features of different realizations that can achieve a similar match to production data. This would greatly improve efficiency, because the changes could be built into the procedure in static model construction.

The algorithm must be automated. The selection of perturbation locations, updating, and iteration must be automated for routine application. Finally, the methodology needs to be applied to other reservoirs.

Iteration	Perturbation Location	
	Selected Partly random, partly on the largest local mismatch	Selected by the largest product of local mismatch and rate mismatch
1st	At Well 1	At Well 1
2nd	Near Well 1	At Well 1
3rd	At Well 4	At Well 4
4th	At Well 8	At Well 1
5th	At Well 4	At Well 1
6th	At Well 3	At Well 8
7th	At Well 1	At Well 8
8th	At Well 1	At Well 3
9th	At Well 4	At Well 3
10th	At Well 5	At Well 1

Table 1. The perturbation location at each iteration related to the two curves in Figure 1.

Iteration	Perturbation Location	
	Gaussian Variogram	Spherical Variogram
1st	At Well 1	At Well 1
2nd	Near Well 1	At Well 1
3rd	At Well 4	At Well 4
4th	At Well 1	At Well 1
5th	At Well 4	At Well 1
6th	At Well 8	At Well 8
7th	At Well 4	At Well 8
8th	At Well 1	At Well 3
9th	At Well 3	At Well 3
10th	At Well 4	At Well 1
11th	At Well 6	At Well 6
12th	At Well 2	At Well 2

Table 2. The perturbation locations for single perturbation at each iteration.

Iteration	Perturbation locations	
	Gaussian Variogram	Spherical Variogram
1st	at Wells 1,3,4,6 and 8	at Wells 1,3,4,6 and 8
2nd	at Wells 1,3 and 4	at Wells 1,3 and 4
3rd	at Wells 1,3 and 4	at Wells 1 and 3
4th	at Wells 1, 3 and 4	at Wells 1, 4 and 8
5th	at Wells 1 and 4	at Well 1
6th	at Well 1	at Well 1
7th	at Well 1	at Well 1

Table 3. The perturbation locations for the multiple perturbations at each iteration.

Well and Perturbation locations
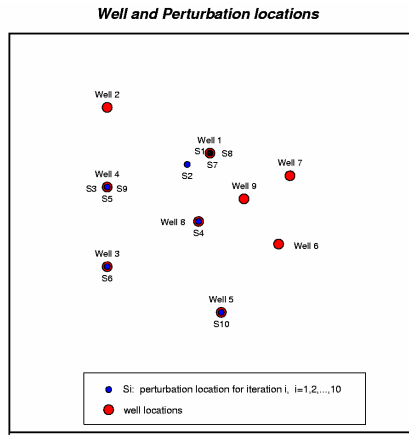
Figure 1. Perturbation locations, selected partly random and partly by the local mismatch at wells.
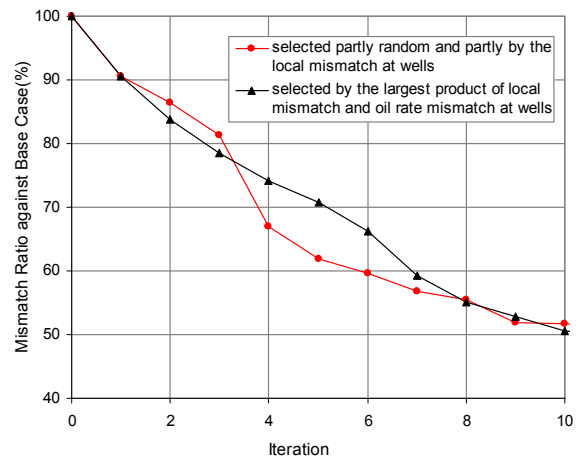
Figure 2. Effect of the selection of perturbation locations.
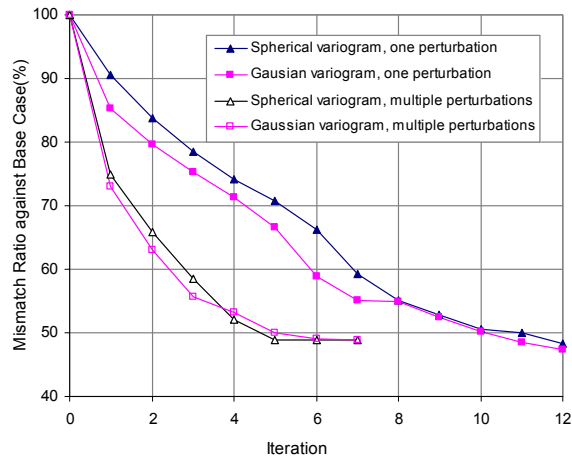
Figure 3. Comparison of global mismatch ratio against the base model between the updated models for different perturbation variogram types.
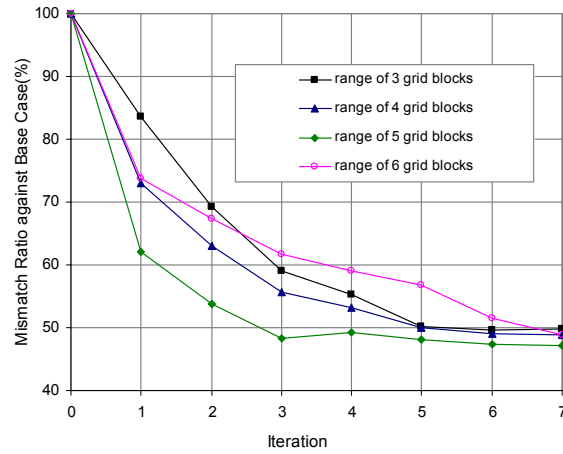
Figure 4. Comparison of global mismatch between the updated models for different perturbation ranges at each iteration.
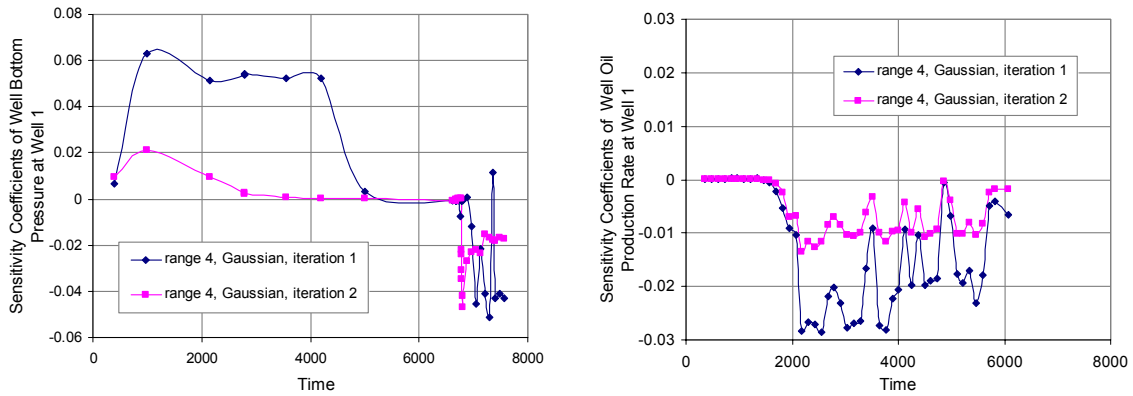
Figure 5. The behavior of sensitivity coefficients of well bottom hole pressure and oil production rate subject to the permeability change at the grid block with Well 1 for the two iterations.
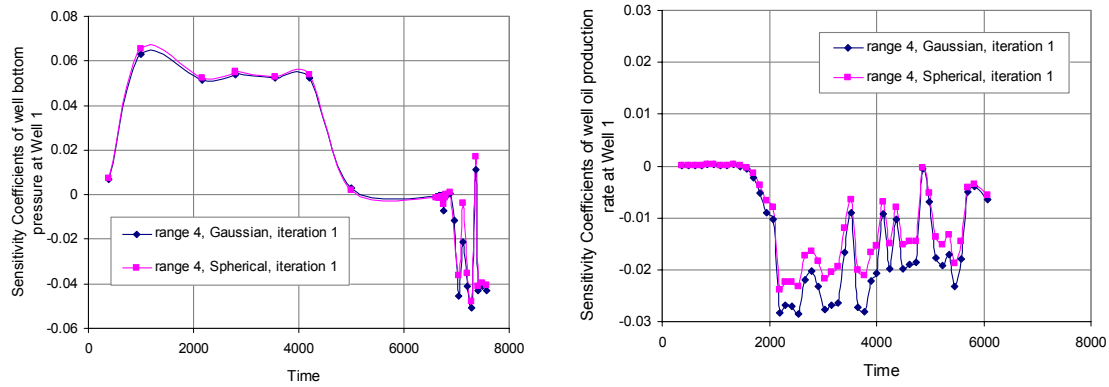
Figure 6. The behavior of sensitivity coefficients of well bottom hole pressure and oil production rate subject to permeability change at the grid block with Well 1 for different perturbation variogram types.
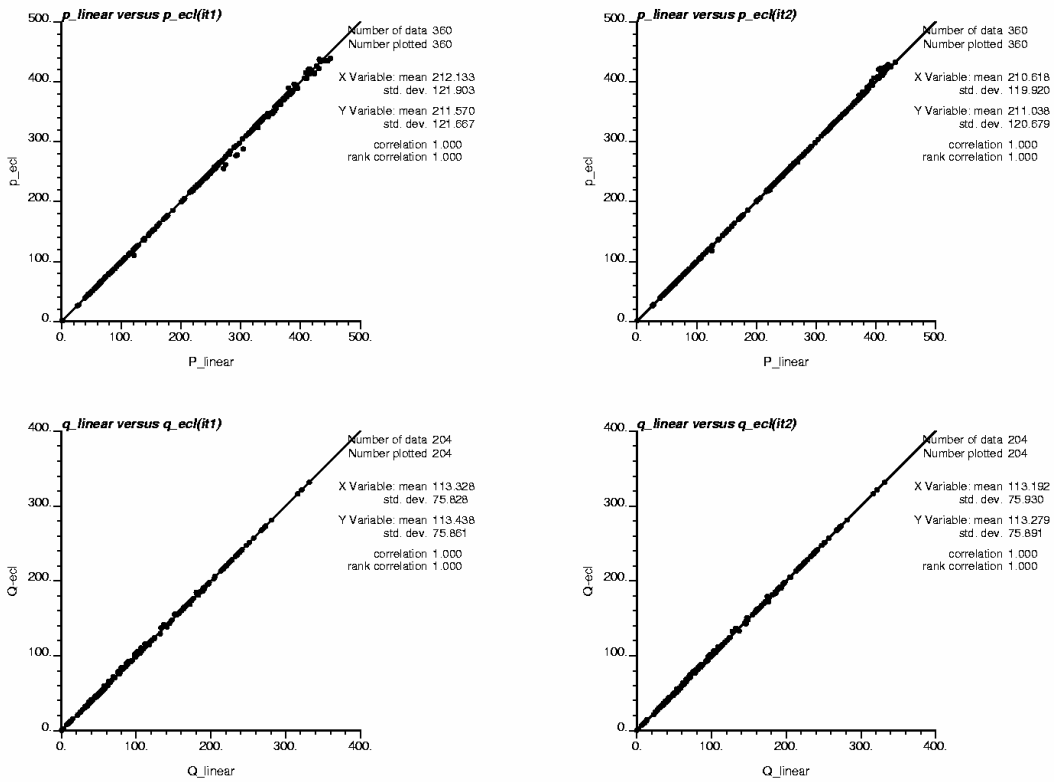
Figure 7. Well bottom hole pressure and oil production rates from the linearized formula and flow simulation. (p_ecl and q_ecl are simulation results; p_linear and q_linear are results calculated from the linear approximation; it1 and it2 mean iteration 1 and iteration 2 respectively)
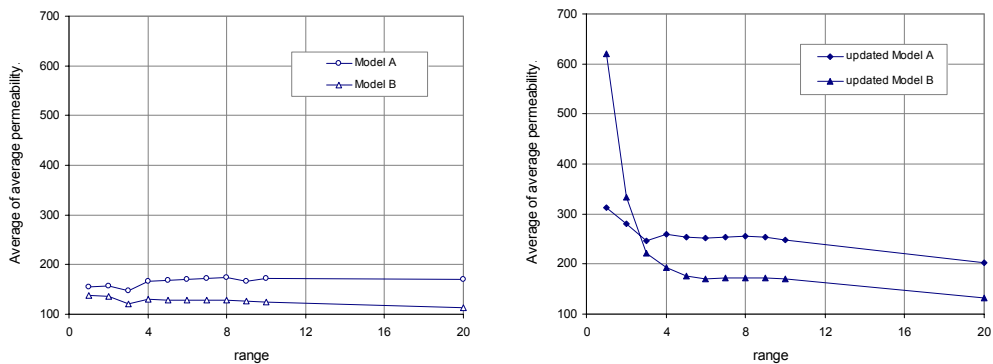
Figure 8. The average values of the average permeability for all wells in the reservoir from the original models and the updated models.